View metadata, citation and similar papers at core.ac.uk

brought to you by CORE

provided by Archive Ouverte en Sciences de l'Information et de la Communication

Toward an Adjoint Based Aeroacoustic Optimisation for Propeller Noise Reduction

Alain Chelius, Itham Salah El Din, Régis Koch

▶ **To cite this version:**

Alain Chelius, Itham Salah El Din, Régis Koch. Toward an Adjoint Based Aeroacoustic Optimisation for Propeller Noise Reduction. ICSV26, Jul 2019, MONTREAL, Canada. hal-02351403

HAL Id: hal-02351403

https://hal.archives-ouvertes.fr/hal-02351403

Submitted on 6 Nov 2019

HAL is a multi-disciplinary open access archive for the deposit and dissemination of scientific research documents, whether they are published or not. The documents may come from teaching and research institutions in France or abroad, or from public or private research centers.

L'archive ouverte pluridisciplinaire **HAL**, est destinée au dépôt et à la diffusion de documents scientifiques de niveau recherche, publiés ou non, émanant des établissements d'enseignement et de recherche français ou étrangers, des laboratoires publics ou privés.

26th INTERNATIONAL CONGRESS ON SOUND AND VIBRATION
7-11 July 2019, Montreal

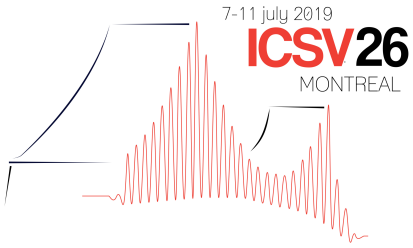

TOWARD AN ADJOINT BASED AEROACOUSTIC OPTIMISATION FOR PROPELLER NOISE REDUCTION

Alain Chelius, Itham Salah El Din and Régis Koch
ONERA - Université Paris Saclay, F-92322 Châtillon, France
email: alain.chelius@onera.fr

The objective of the work described in this paper is to set up and validate an adjoint based method for blade shape optimisation aiming at propeller noise reduction. As a first step toward a comprehensive propeller noise optimisation, the present study focuses on the loading noise of a single propeller isolated and without incidence. In this respect, an acoustic objective function is derived, based on the Hanson-Lévy steady loading noise formulation. After defining this function, the first step is to derive its sensitivities to mesh and aerodynamic field parameters. Once implemented in the ONERA adjoint based optimisation procedure, the acoustic function predictions are compared to a classical Ffowcs Williams and Hawkings approach, and the sensitivities are validated by comparison with the finite differences method.

Keywords: blade shape optimisation, aeroacoustic objective

1. Introduction and motivation

Once the blade shape of a propeller has been designed to comply with targeted aerodynamic performances, reducing its noise generally requires parameter modifications which are antagonistic with the aforementioned performances. For instance, reducing the diameter or the regime mitigates the emitted noise thanks to the tip Mach number reduction, but requires an adaptation of the blades pitch angle to maintain sufficient thrust. Thus, the acoustic mitigation is constrained by the aerodynamic performances. In addition, the acoustic and aerodynamic impacts of local blade shape modifications are difficult to foresee, and a trial-and-error approach based on Computational Fluid Dynamics (CFD) and Computational Aero-Acoustics (CAA) simulations is time consuming. Therefore, blade shape optimisation based on aero-acoustic criteria appears as an alternative approach to this engineer-made design, since modern optimisation techniques may quickly lead to non-contemplated solutions. This is why in this paper we focus on a gradient optimisation with adjoint method applied to propeller noise reduction.

More exactly, this work deals with the case of an isolated single propeller without incidence, since it provides an appropriate framework to validate the method. Indeed, the steady behavior of the flow in the rotating blade frame allows first to rely on steady CFD and adjoint strategies, and then to compute the radiated tonal noise with a frequency domain approach. In this respect, we define an acoustic objective function based on the Hanson-Lévy steady loading noise formulation. Thus, the objective of the present work is to set up and validate this method, based on the RANS adjoint solver of ONERA CFD code *elsA* [1, 2].

The first part of this paper addresses the theoretical aspects of the work, first briefly presenting the adjoint method, and then detailing the formulation of the acoustic objective function and how its sensitivities to the mesh and flow field are obtained. The second part introduces the propeller application case and its numerical set up, and the third section demonstrates the method validity, checking first the acoustic function reliability, and then its sensitivities evaluation.

2. Aeroacoustic adjoint for propeller noise

2.1 The discrete adjoint method

Aerodynamic shape optimisation consists in looking for a set of shape parameters $\alpha = (\alpha_1, ..., \alpha_{n_f})$ that minimizes a given objective function J under n_c constraint functions G_k, with $k \in [1, n_c]$. These objective and constraints functions depend on the geometry and the aerodynamic flow. The latter is described by the discretized equations of fluid mechanics, of residual $R(W, X) = 0$, where W represents the aerodynamic state variables, and X the mesh of the computational domain. Gradient-based optimisation methods consist in iteratively compute the flow W for a given shape α, evaluate the functions and their gradients with respect to this shape $dJ/d\alpha$ and $dG_k/d\alpha$, define a new shape parameter vector by applying a descent algorithm, and finally mesh a new shape and a new computational domain. There are several methods to compute the above gradients, the discrete adjoint being one of them. It relies on the linearised equation:

$$\frac{dJ}{d\alpha} = \frac{\partial J}{\partial X}\frac{dX}{d\alpha} + \lambda^T \left(\frac{\partial R}{\partial X}\frac{dX}{d\alpha} \right) \tag{1}$$

with the adjoint vector λ such that $\lambda^T = -\frac{\partial J}{\partial W}\left(\frac{\partial R}{\partial W}\right)^{-1}$, i.e. solution of the discrete adjoint equation:

$$\frac{\partial J}{\partial W} + \lambda^T \frac{\partial R}{\partial W} = 0 \tag{2}$$

The evaluation of the gradient, based on Eqs. (1) and (2), requires the knowledge of the terms $\frac{\partial J}{\partial X}$ and $\frac{\partial J}{\partial W}$, the function sensitivities to the mesh and flow respectively. They can be explicitly linearised, as is done for the aeroacoustic function in Section 2.2.3. The mesh sensitivity to the shape parameters $\frac{\partial X}{\partial \alpha}$ may be obtained either numerically or with finite differences, depending on the meshing tools used. An extensive description of the discrete adjoint approach can be found in [3].

2.2 The propeller noise function

Aerodynamic sound origins are usually splitted in three terms: thickness noise, related to the volume displacement of moving solid boundaries, loading noise, due to the forces exerted by solid surfaces on the fluid, and quadripolar noise, generated by sources in the flow. In the case of an isolated subsonic propeller, noise is mainly tonal (in opposition to broadband noise) and due to both thickness and loading noise. In the present work, as a first step toward an exhaustive propeller acoustic optimisation, it has been chosen to focus only on the latter noise component. This choice is maintained by the fact that on modern designs, and in most operating conditions, loading noise is the dominant source. Moreover, the linear nature of the three type of sources (see [4], Eq. (3.6) for instance) allows to consider the other terms in future works.

2.2.1 Steady loading noise formulation

Let us consider an orthonormal frame $Oxyz$ in translation at uniform velocity $U = c_\infty M$ along the x axis, c_∞ being the speed of sound and M the Mach number. According to [5], the loading noise sound

pressure at a point $\overrightarrow{x}(x_1, x_2, x_3)$ at time t is the following:

$$p(\overrightarrow{x}, t) = \int_S \int_\tau F_i \frac{\partial G}{\partial y_i} d\tau dS \tag{3}$$

where S is the propeller blades surface, τ the emission time, F_i (i = 1,2,3) the components of the force per surface element exerted on the fluid, $\overrightarrow{y}(y_1, y_2, y_3)$ the location of the sources, and $G(\overrightarrow{y}, \tau; \overrightarrow{x}, t)$ the Green function in uniform velocity field. This equation may be solved either in the time domain, as in [5], or in the frequency domain. The latter is selected for this study since it allows to relate the loading noise to quantities such as thrust and torque, which have been previously linearised and implemented in the ONERA optimisation chain [6, 7]. Integration of Eq. (3) in the frequency domain has been performed by Hanson [8] and Lévy [9, 10], which only differ by their choice of reference frame. In the following we take the Lévy approach, solving the equation in the frame translating with the propeller, though we refer to the Hanson-Lévy formulation.

For a B blades propeller, rotating at the angular velocity $\Omega = 2\pi N$ in the yOz plane, the Fourier transform of Eq. (3) leads to the pressure at the harmonic frequencies of the rotation mB, i.e. multiples of order m of the Blade Passing Frequency (BPF). With a far field assumption, i.e. the observation distance is large compared to the source dimensions and the emitted wavelength, it is shown in [9] that the loading noise can be written:

$$P(mB, \overrightarrow{x}) = \frac{ikB}{4\pi S^2} e^{-ik\sigma} \sum_{s=-\infty}^{+\infty} e^{-i(mB+s)(\phi-\pi/2)} \cdot \int_S \left[\left(\frac{MS + x_1}{\beta^2} \right) f_1^{(s)} + x_2 f_2^{(s)} + x_3 f_3^{(s)} \right] . e^{i(kA_1 - mB\psi_c)} \mathcal{J}_{mB+s}(kA)\, dS \tag{4}$$

In this expression the cylindrical coordinates of $\overrightarrow{x}$ and $\overrightarrow{y}$ are respectivley (d, ϕ, x_1) and (r, ψ, y_1), integration is now over the surface S of a single blade, $k = \frac{2\pi mBN}{c_\infty}$ is the wavenumber, $\beta = \sqrt{1 - M^2}$, $S = \sqrt{x_1^2 + \beta^2 (x_2^2 + x_3^2)}$, $\sigma = \frac{Mx_1 + S}{\beta^2}$, $A = \frac{rd}{S}$, $A_1 = \frac{y_1}{\beta^2}\left(M + \frac{x_1}{S}\right)$, ψ_c expresses the chord non-compactness through the relation $\psi = 2\pi N\tau + \psi_c$, $\mathcal{J}_n$ is the first kind Bessel function of order n, and $f_i^{(s)}$ are the forces harmonics of order s from the Fourier series decomposition of F_i. As stated in the previous paragraph, it is interesting to replace the latter by introducing the thrust T and torque Q per surface element. In the blade frame, the force locally exerted by the blade on the fluid is decomposed into an axial force along the propeller axis, the thrust, a tangential component equal to Q/r and a radial one. Thus, by decomposing the F_i components in the blade frame and neglecting the radial force, one can show that the bracketed term in Eq. (4) becomes:

$$F^{(s)} = -T^{(s)} \frac{MS + x_1}{\beta^2} + Q^{(s)} \frac{mBS}{kr^2} \tag{5}$$

The Sound Pressure Level (SPL) associated to each tone is then $L_p(mB, \overrightarrow{x}) = 10.log\left(\frac{{p_{rms}}^2}{{p_r}^2}\right)$, with $p_r = 2.10^{-5}$ Pa the reference pressure and $p_{rms} = \sqrt{2}|P(mB, \overrightarrow{x})|$ the Root Mean Square amplitude of the tone.

2.2.2 The acoustic objective function

In order to define the acoustic objective function for the optimisation problem, simplifications are made thanks to the fact that the propeller is isolated and without incidence. First, as the blade loads

are steady, the Fourier decomposition of $F^{(s)}$ is limited to the mean term $F^{(0)}$ and the summation over s can be removed from Eq. (4). Second, knowing that the steady loading noise of a propeller radiates its maximum noise in the propeller plane, it is chosen to focus the objective function on an observation point in this plane, i.e. for which $x_1 = 0$. Moreover, this radiation is axisymmetrical, therefore we chose $\phi = \pi/2$ for the sake of simplifications. As a result, $x_2 = 0$ and $x_3 = d$. Then, we chose to focus the objective function on one tone only, the fundamental $m = 1$ being the best candidate for noise reduction since in the case of single isolated propeller it dominates the spectrum. However, the index m is kept in the equations so the optimisation may be tested on the harmonics. Finally, one may notice that once the observation point and the BPF of interest are fixed, the factors in front of the integration term of Eq. (4) are constant, so they will not be taken into account in the objective function.

The integration over the blade surface S is obtained from its discretization by the CFD mesh, by summing the contributions of all the surface cells S_i. Thus, taking into account the previous simplifications leads to an expression proportional to the acoustic pressure of Eq. (4):

$$P_s(mB, \overrightarrow{x}) = \sum_{S_i} \left[e^{i\left(\frac{ky_1M}{\beta^2} - mB\psi_c\right)} . \mathcal{J}_{mB}(kA) dF_i \right] \tag{6}$$

where dF_i is the elementary steady loading force, related to the elementary steady thrust dT_i and torque dQ_i by the relation:

$$dF_i = dT_i \frac{MS}{\beta^2} - dQ_i \frac{mBS}{kr^2} \tag{7}$$

The definitions of dT_i and dQ_i rely on the axial component of the pressure and friction forces exerted on the blade surface element and are detailed in [6].

Finally, the goal of the optimisation being to reduce the SPL of the propeller, the acoustic objective function J is defined in ratio of the square of the tone RMS $J = |P_s(mB, \overrightarrow{x})|^2$, that we prefer to express with $\overline{P_s}$ the conjugate of P_s:

$$J = P_s(mB, \overrightarrow{x}).\overline{P_s}(mB, \overrightarrow{x}) \tag{8}$$

2.2.3 Mesh and flow sensitivities

As explained in Section 2.1, the adjoint method requires to calculate the objective function sensitivities with respect to the mesh X and flow W. It depends naturally on the analytical expression of $J(W, X)$, but also on the data format used by the adjoint solver. In the case of ***elsA***, the flow is represented by the conservative variables (ρ, ρu, ρv, ρw, ρE) at the center of the cells and at the center of surface boundary cells. Thus, these latter points correspond to the acoustic source locations $\overrightarrow{y}$. Based on the definition of the acoustic function given by Eqs. (6, 7, 8), one notices that it depends only on the mesh and field adjacent to the blade surface. More precisely, the exponential and Bessel terms of P_s depend only on the mesh coordinates at the blade surface, noted $X_b(x_b, y_b, z_b)$, while the elementary force dF_i also depends on the first sheet of mesh in the fluid "parallel" to the surface one, noted X_p, on the field at the center of the surface boundary cells, noted W_b, and the field in the cells adjacent to the blade surface, noted W_c. Therefore, the sensitivities of the acoustic function $J(W, X)$ are given by the following differentiations:

$$\frac{\partial J}{\partial X_{b/p}} = \left(\frac{\partial J}{\partial x_{b/p}}; \frac{\partial J}{\partial y_{b/p}}; \frac{\partial J}{\partial z_{b/p}} \right)^T, \quad \frac{\partial J}{\partial W_{b/c}} = \left(\frac{\partial J}{\partial \rho_{b/c}}; \frac{\partial J}{\partial \rho u_{b/c}}; \frac{\partial J}{\partial \rho v_{b/c}}; \frac{\partial J}{\partial \rho w_{b/c}}; \frac{\partial J}{\partial \rho E_{b/c}} \right)^T.$$

These expressions, not detailed here for the sake of brevity, are obtained analytically by hand chain derivation, with the same method and notations as in [6], in which $\partial dF_i/\partial(X|W)$ and $\partial dQ_i/\partial(X|W)$ have already been developped. It is then implemented in the in-house tool ***HeliOpt***.

3. Propeller noise problem

3.1 Configuration

The propeller used in this work cannot be shown and only few details can be given for confidentiality reasons. It is a full scale five blades puller propeller designed for short-range flight aircrafts. In the present case, the operating condition is a cruise flight without incidence, for which some data is provided in Table 1. The propeller is isolated, however the geometry includes the spinner and the hub.

Table 1: Propeller cruise condition characteristics.

Parameter	Value
Number of blades B	5
Flight Mach number M	0.50
Rotation regime [rpm]	1500
Thrust coefficient C_T	0.22
Static pressure p_∞ [Pa]	26436.3
Sound velocity c_∞ [m.s^{-1}]	299.463

3.2 Numerical set up

The CFD simulations rely on ONERA's finite volume solver *elsA* [11]. Since the present case is axisymmetrical, it allows to limit the computational domain to one blade channel of azimuthal extent $2\pi/B$, as illustrated in Fig. 1. As already stated, the flow is steady in the blade frame, therefore the computations are performed in this rotating frame by solving the steady compressible Reynolds-Averaged Navier-Stokes (RANS) equations. The mesh is built with structured full matching multiblocks, extending $10R$ up and downstream from the blade pitch axis and radially, R being the blade radius. The whole mesh is approximately 6 million points.

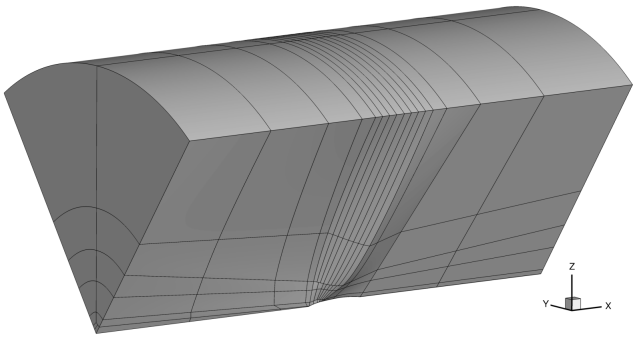

Figure 1: Mesh blocks of the CFD domain

The RANS equations are closed using the Spalart-Allmaras turbulence model [12]. The reason for chosing this model is that it is so far the most advanced turbulent model that has been linearised in the *elsA* adjoint solver, and it is desirable to apply the same numerical schemes in both CFD and adjoint solvers to ensure the optimisation process robustness. The convective fluxes are discretized with a Roe upwind scheme [13] with MUSCL extension to the second order and a van Albada limiter [14]. The diffusive fluxes are discretized using a second order centered scheme. The time marching scheme is a first order backward Euler.

4. Method validation

4.1 Acoustic function

As a first step toward validation of the optimisation strategy, the loading noise function implementation has to be validated. For that purpose, the Ffowcs Williams and Hawkings method (FWH) is considered as a reference, using the well validated in-house code *KIM* [15], based on blade pressure extracted from the CFD. The acoustic function is not directly comparable to the Sound Pressure Level obtained by FWH, since it is a simplified form of the Hanson-Léwy SPL (cf. Section 2.2.1). Therefore, the latter is considered rather than J in order to perform such comparisons. Directivities along a semi-arc

at $73.8R$ in a plane perpendicular to the propeller one are shown on Fig. 2. In the downstream direction, i.e. over $\theta = 90°$, both formulations present similar directivities whatever the tone frequency, with an underestimation by Hanson-Lévy between 1 and 2 dB. Below $90°$, it overestimates the FWH predictions up to 17 dB. The far field hypothesis made on the Hanson-Lévy formulation is respected, thus it cannot be the cause of such large differences, and it seems unlikely that the radial forces on the blade, which are neglected, can have such an impact. These discrepancies are still investigated. However, one may note that the BPF levels at $\theta = 90°$, which has been chosen as the noise level to be evaluated by the J function and reduced through the optimisation, are in satisfying agreeement with a 0.9 dB difference.

The SPL at this particular tone and direction is further investigated. Three shape parameters of blade profile, sweep, chord length and maximum thickness, are modified in order to induce a local blade deformation at $0.75R$. Each deformation produces a new blade geometry, which is simulated by CFD and acoustically evaluated with *KIM* and the acoustic function J. Figure 3 presents the SPL variations compared to the original blade shape for six deformation cases. Although the noise variations are very small (below 0.1 dB), the acoustic function shows trends similar to the FWH results, thus validating the acoustic function ability to reflect the loading noise sensibility to shape variations. In other words, if the optimisation procedure manages to mitigate J, it will mitigate the far field loading noise accordingly.

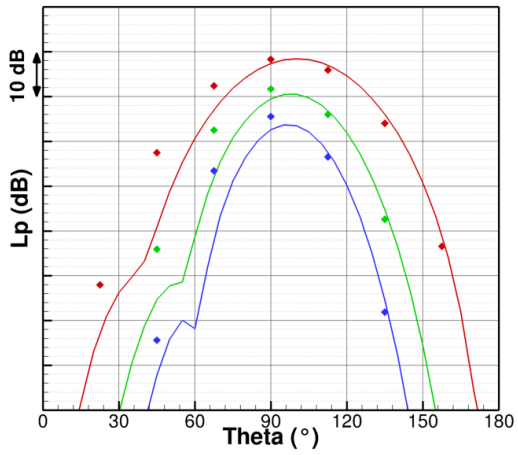

Figure 2: Far-field loading noise directivities calculated with *KIM* (—) and the Hanson-Lévy formulation (◆), for BPF, 2BPF and 3BPF.

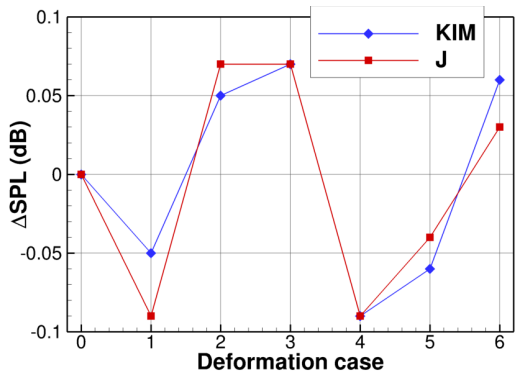

Figure 3: Loading noise SPL variations obtained by *KIM* and the acoustic function J, at the BPF and in the propeller plane, with local blade deformations: 0: no deformation; 1-2: sweep $\pm 2°$; 3-4: chord $\pm 2\%$; 5-6: thickness $\pm 2\%$

4.2 Sensitivities

The acoustic function sensitivities $\frac{\partial J}{\partial X}$ and $\frac{\partial J}{\partial W}$ developped in 2.2.3 and computed by *HeliOpt* are now compared to values obtained with second order finite differences. The latter consist in adding a local small perturbation to the field or flow. For instance, for the sensitivity to x_b on the node i, we calculate:

$$\frac{\partial J}{\partial x_{b,i}} \approx \frac{J(W(\alpha), X_{+\delta x_{b,i}}(\alpha)) - J(W(\alpha), X_{-\delta x_{b,i}}(\alpha))}{2\delta x_{b,i}} \tag{9}$$

where $X_{\pm\delta x_{b,i}}$ represents the initial mesh X perturbed by $\pm\delta x_{b,i}$ on coordinate x_b of node i. The perturbation amplitude is chosen depending on the studied variable local variations. For instance, for $x_{b,i}$ the $\delta x_{b,i}$ amplitude has to be very small compared to $|x_{b,i\pm1} - x_{b,i}|$.

Some results are presented on Fig. 4, for the sensitivites to x_b and ρ_b. These values are computed on grid points or cell centers on the blade surface along a section close to the tip, where load sources

are known to be the strongest. The results given by the analytical formulae implemented in *HeliOpt* are in excellent agreement with those obtained by finite differences. Similar results are obtained for all the variables of X_b, X_p, W_b and W_c, as well as for a section at the blade root ($0.36R$). Therefore, the acoustic function sensitivities to the mesh and flow are validated.

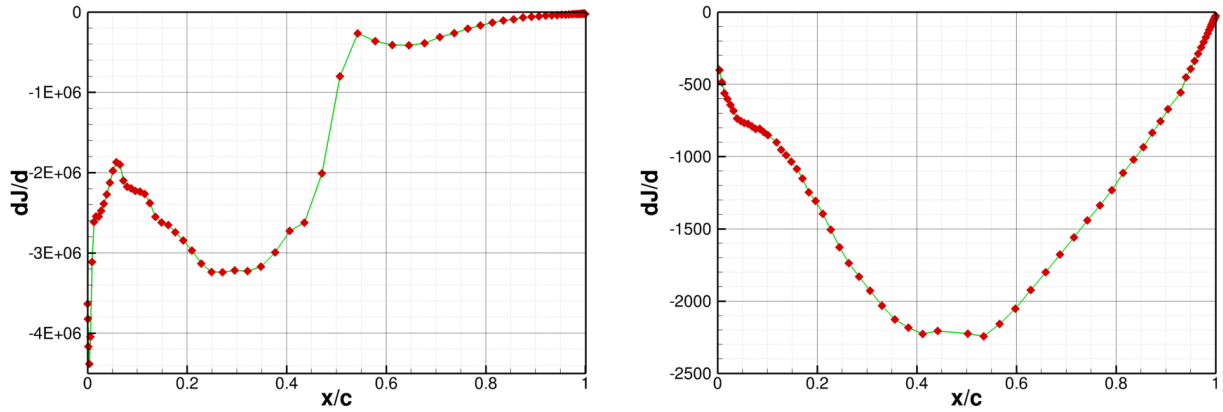

(a) $\frac{\partial J}{\partial x_b}$, suction side

(b) $\frac{\partial J}{\partial \rho_b}$, pressure side

Figure 4: Sample of acoustic function mesh and flow sensitivites calculated by *HeliOpt* (—) and finite differences (♦) on a blade section at $0.82R$.

5. Conclusions and prospects

This study proposes a first approach of adjoint based shape optimisation for propeller noise reduction, and lays the foundation required for that method. The frame of a single subsonic propeller without incidence offers an ideal case for steady adjoint, and allows to focus the acoustic analysis on steady loading noise. Therefore the latter is defined as the objective function that must be minimized, and this acoustic function is derived from the Hanson-Lévy formulation. The sensitivities to the mesh and flow, required for the adjoint solving, have been linearised by hand. Beforehand performing a blade shape optimisation based on this objective, the function is compared to FWH noise simulations on a propeller test case. Although there are discrepancies in the upstream direction, the general trends of the SPL in the propeller plane are correctly predicted, especially the noise variations when changing local shape parameters. Then, the function sensitivities are compared to evaluations realised by finite differences, showing excellent agreement. Therefore, the implementation of the acoustic function and its sensitivities in the optimisation process are validated.

The next step of this work is to chose relevant shape parameters for the optimisation, and validate the gradients calculated by the adjoint solver against finite differences. This exercice is currently on going at ONERA on sweep, chord length and maximum thickness. There are many other approaches for parametrising this optimisation problem, among which the free-form method [16] is also contemplated for future work. Then, an optimisation may be performed. However, it requires to define a strategy, including the above parametrisation, but also the constraint functions, which in the present case are likely to be the propeller thrust and/or power, since we want to maintain a certain level of aerodynamic performance. The challenge is to foressee what is the most suited strategy that will lead to the best optimisation, i.e. maximum noise mitigation with minimum performance loss.

Acknowledgments

Part of this work has been done in the frame of the project MADELEINE and has received funding from the European Union's Horizon 2020 research and innovation programme under Grant Agreement No 769025.

REFERENCES

1. Peter, J. Discrete adjoint method in elsa (part 1): method/theory, *7th ONERA-DLR Aerospace Symposium*, (2006).
2. Carrier, G., Mouton, S. and Salah El Din, I. Discrete adjoint method in elsa (part 1): Application to aerodynamic design optimisation, *7th ONERA-DLR Aerospace Symposium*, (2006).
3. Peter, J. and Dwight, R. Numerical sensitivity analysis for aerodynamic optimization: A survey of approaches, *Computers and Fluids*, **39**, 373–391, (2010).
4. Goldstein, M. E., *Aeroacoustics*, McGraw-Hill International Book Company, New York (1976).
5. Ffowcs Williams, J. E. and Hawkings, D. L. Sound generation by turbulence and surfaces in arbitrary motion, *Phil. Trans. R. Soc. Lond. A*, **264** (1151), 321–342, (1969).
6. Dumont, A., *Calculs de gradients pour l'optimisation des performances aérodynamiques d'un rotor d'hélicoptère en vol stationnaire.*, Ph.D. thesis, Faculté des Sciences Fondamentales et Appliquées, Université de Poitiers, (2010).
7. Dumont, A., Le Pape, A., Peter, J. and Huberson, S. Aerodynamic shape optimization of hovering rotors using a discrete adjoint of the reynolds-averaged navier-stokes equations, *Journal of the American Helicopter Society*, **56**, 032002–1–11, (2011).
8. Hanson, D. B. Helicoidal surface theory for harmonic noise of propellers in the far field, *AIAA Journal*, **18** (10), 1213–1220, (1980).
9. Léwy, S. Prévision du bruit de raies émis par un rotor : application à l'aéronautique, *Journal de Physique*, **4**, C5–55 – C5–65, (1994).
10. Léwy, S. Prediction of tone noise radiated by transonic axial flow fans, *3rd International Congress on Air- and Structure-Borne Sound and Vibration*, (1994).
11. Cambier, L., Heib, S. and Plot, S. The Onera elsA CFD software: input from research and feedback from industry, *Mechanics and Industry*, **14**, 159–174, (2013).
12. Spalart, P. R. and Allmaras, S. R. A one-equation turbulence model for aerodynamic flows, *30th AIAA Aerospace Sciences Meeting and Exhibit*, (1992).
13. Roe, P. L. Approximate riemann solvers, parameters vectors and difference schemes, *J. Comput. Phys.*, **43**, 357–372, (1981).
14. van Leer, B. Towards the ultimate conservative difference scheme, v. a second order sequel to godunov's method, *J. Comput. Phys.*, **32(1)**, 101–136, (1979).
15. Prieur, J. and Rahier, G. Aeroacoustic integral methods, formulation and efficient numerical implementation, *Aerosp. Sci. and Technology*, **5**, 457–468, (2001).
16. Dumont, A., Méheut, M., Baumgärtner, D. and Bletzinger, K.-U. Aerodynamic shape optimization progress on adodg benchmark problems using the elsa software, of Aeronautics, A. I. and Astronautics (Eds.), *35th AIAA Applied Aerodynamics Conference*, pp. AIAA 2017–4081, (2017).